Pre-failure damage, time-dependent creep and strength variations of a brittle granite

O. Katz
Institute of Earth Sciences, Hebrew Univ., Jerusalem, and Geological Survey of Israel, Jerusalem, Israel

Z. Reches
Institute of Earth Sciences, Hebrew Univ., Jerusalem, Israel

ABSTRACT: We experimentally analyze the effects of stress-induced damage and time-dependent creep on the brittle failure of Mount Scott granite of Oklahoma. Fourteen dry granite samples were tested at room temperature and under 41MPa confining pressure; they were loaded to a pre-selected axial stress and held under a constant stroke for periods of up to six hours before unloading. The majority (80%) of the microfractures mapped in thin-sections belong to two groups: tensile fractures that subparallel the loading axis, and shear fractures trending 15°-40° off the loading axis. The analysis indicates (a) that samples loaded above a critical stress (about 0.96 the mean strength) creep under constant stroke and relaxing stresses during the hold period and eventually fail spontaneously; and (b) that the strength variations of the samples fit Weibull distribution with profound weakening due to the creep.

1 INTRODUCTION

Stressing brittle rocks leads to the development of distributed damage long before the rock fails unstably. The damage is commonly manifested by microfractures and dilational microcracks (Brace & Tapponier, 1976). Typically, these microfractures are smaller than the grain size and they are often quasi-uniformly distributed prior to faulting (Hadely, 1976; Lockner et al. 1992). Local, non-uniform distributions of microfractures are related to fault nucleation and growth (Reches & Lockner, 1994). The microdamage was used to explain the reduction of seismic wave velocity, seismic anisotropy, the reduction of elastic moduli and strength, and the mechanics of rock failure (Ashby & Hallam, 1986, Reches & Lockner, 1994, Lyakhovsky et al. 1997; Lockner, 1998). Further, the stress-induced damage may facilitate time-dependent creep driven by stress corrosion and subcritical crack growth (Lockner, 1998). This creep strongly affects the long term strength and failure stability. For example, granite samples subjected to one month of constant, uniaxial stress could fail under stress of ~0.65 the instantaneous strength (Schmidtke & Lajtai, 1985). Or, "delayed fractures" could develop days to years after the applied loads were removed (Salganik et al. 1994).

We examine here the pre-failure damage and rock strength in triaxial experiments of brittle granite samples. The stress-induced damage was determined from both rheological parameters and microfracturing analysis (Katz, 2002). The load-hold method is applied here to recognize the time-dependent damage in the tested brittle granite. The stress distribution results are analyzed following Lawn (1993, Ch. 10) who discussed the lifetime of material under load below the inert strength level in terms of fatigue and crack growth velocity function.

The present experimental work was conducted at the Rock Mechanics Institute, University of Oklahoma, Norman, Oklahoma, and the experimental details appear in Katz (2002). In this paper, we briefly outline the experimental procedure and describe the macroscopic rheology and microstructural observations. Then, we discuss the effects of the instantaneous damage and time-dependent damage on the strength of the granite.

2 EXPERIMENTAL PROCEDURE

2.1 Experimental set up

We used samples of Mount Scott granite (MSG) of the Wichita Mountains, southwestern Oklahoma. MSG has anorthoclase phenocrysts in a matrix of alkali feldspar and quartz with small amounts of hornblende, biotite and iron oxides (Price et al. 1996). It is a fine- to medium-grained rock with mean grain size of 0.9±0.2mm and dry density of 2,645kg/m3. Katz et al. (2001) conducted a series of thirteen uniaxial and triaxial loading-to-failure tests under confining pressure up to 66MPa. They found that the Young's modulus, E, increases from 75GPa for the

uniaxial tests, to 82GPa at 66MPa confining pressures, and the Poisson's ratio is 0.21 - 0.31. The Coulomb strength of MSG is $\sigma_1 = 270 + 8.7\sigma_3$ (in MPa), and the measured angle θ between the normal to the major faults and the sample axis (σ_1) is 68º - 75º (Katz et al. 2001).

The present tests were performed on 25.4mm diameter cylinders with length-to-diameter ratio of 2.5 –3.9. We used a 69MPa pressure vessel and the axial load was supplied by a servo-controlled hydraulic load frame (MTS 315). Load was monitored with an internal load cell, and the displacements were monitored with two LVDT (axial), and a chain extensometer (lateral). All tests were performed under the confining pressure of 41MPa for which the Coulomb strength is 586±16MPa (Katz et al. 2001). We define the 'Normalized Differential Stress', NDS, as NDS = $(\sigma_1 - \sigma_3) / 586$. While ideally the maximum NDS = 1.0, in our tests 0.96 < maximum NDS < 1.05, reflecting the inherent inhomogeneity of the samples and deviations from mean strength.

2.2 Loading procedure

We use three loading procedures:

1. Load-to-failure at axial strain rate of $1 \cdot 10^{-5}$ s^{-1}, after the confining pressure loading at a constant rate of 0.023MPa/s. This procedure was used for tests 101, 103, 112.
2. Load-hold procedure applied in 14 tests (Table 1), each consists of four steps:

(a) Confining pressure loading at a rate of 0.023MPa/s;

(b) Axial loading to a pre-selected load that ranges from NDS = 0.54 to NDS = 1.05. Axial shortening was at a strain rate of $1 \cdot 10^{-5}$ s^{-1};

(c) Once the pre-selected load was achieved, the specimen was held at a constant stroke for up to six hours;

(d) Eleven samples did not fail during the hold time and three failed spontaneously. After the hold period, the unfailed samples were unloaded.

3. Cycle-to-failure procedure was applied on three unfailed samples (105, 124 and 125). The axial load was unloaded (to the confining pressure) after the holding period and the sample was reloaded to failure in one or two cycles.

3 EXPERIMENTAL OBSERVATIONS

3.1 Stress-strain relations

The stress-strain curves of test 101 (Fig. 1) are characteristic for the present experiments. Figure 1 displays the axial strain curve (with diamonds indicating the pre-selected holding stresses), the experimental volumetric strain, ΔV/V, and the permanent volumetric strain, CSV. The later is associated with crack dilation where CVS=[(experimental volumetric strain)-(elastic volumetric strain)], or

$$CSV = (\sigma_1 - \sigma_3)(1-2\nu)/E.$$

The curves display several stages that are similar to previously recognized stages (Wawersik & Brace, 1971). Stage I, at the range of 0< NDS< 0.15, includes the nonlinear stress increase associated with cracks closure. Stage II, at 0.15< NDS< 0.40, displays apparently linear elastic curve. Stages III and IV start at NDS ≈ 0.4 (C_{ci} – crack initiation stress, Martin & Chandler, 1994) and NDS ≈ 0.85 (C_{cd} – crack damage stress, Martin & Chandler, 1994), respectively, are characterized by first stable (stage III) and then unstable (stage IV) crack growth and dilation. Stage V is the failure stage (NDS ≈ 1.0) during which the sample failure occurred by initial stable stress decrease followed by unstable stress drop.

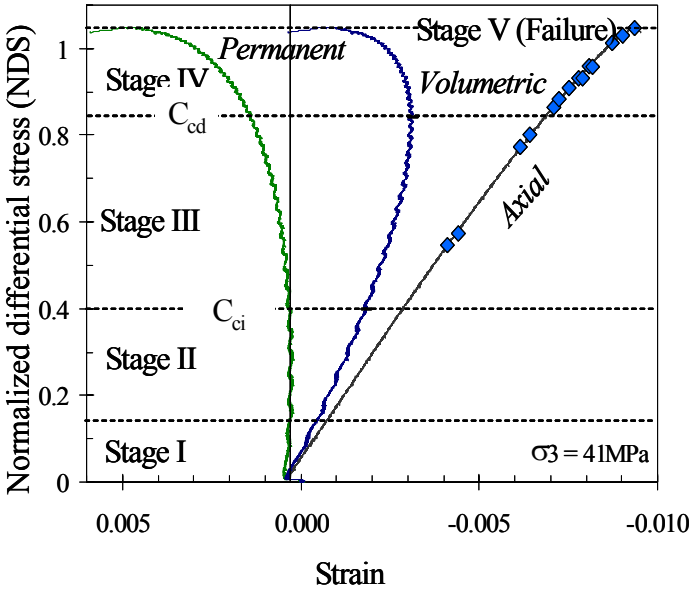

Figure 1. Stress-strain relations of test 101. Stress axis is marked by Normalized Differential Stress (NDS, see text). The shown curves are: axial load, total volumetric strain and permanent, crack volumetric strain (CVS, see text). The curves display several stages (after Wawersik and Brace, 1971): I- nonlinear stress increase associated with cracks closure; II- quasi-linear elastic stage; III- nonlinear stress increase associated with crack growth and dilation; IV- failure stage with increase of crack growth; V-failure. C_{ci} is the crack-initiation stress, where dilation begins; C_{cd} is the crack-damage stress, where failure initiates. Diamonds represents the maximal NDS of each of the load–hold test in the present series.

3.2 Time-dependent creep

Time-dependent effects of damage evolution are recognized in the holding periods. During the holding period the sample length was maintained constant and the axial stresses could relax spontaneously. In this respect, the present procedure differs from typical creep test in which the stress level is constant and the sample is allowed to shorten. The holding periods did not exceed six hours due to limited availability of the loading frame.

All eleven samples with maximum loading of NDS < 0.96 did not fail spontaneously during the hold periods. These samples exhibit similar variations of the axial stress, volumetric strain and crack volumetric strain that are similar to the relations in Figure 1. During the hold period, the axial stress of these samples relaxes first by 2-3% and remains approximately constant thereafter (test 113 in Fig. 2).

Different behavior is observed for the three samples loaded with NDS ≥ 0.96 in the holding stage (tests 104, 106 and 110, Table 1). In these tests, the axial stress relaxed during the hold time until they fail spontaneously (Fig. 2). The irregular relaxation curves indicate poorly constrained creep processes that are probably associated with stress corrosion or subcritical crack growth.

Table 1. Experimental loading data. Loading procedure includes: load to failure tests (specimens 101, 103, 112); load-hold tests (specimens 102, 104, 105, 106, 108-110, 113-117, 123, 125); cyclic loading to failure tests (specimens 105, 124, 125); Hold time: the time elapsed from start of stroke holding to unloading or to failure; Hold stress is the maximum stress at the start of holding; Maximum NDS: is the normalized differential stress at hold point or at failure.

Test #	Hold time min	Hold stress (MPa)	Failure stress (MPa)	NDS	Comments
101	-	-	613	1.05	load to failure
102	95	601	-	1.03	Load-hold
103	-	-	595	1.02	load to failure
104	61	613	528	1.05	spontaneous failure
105	180	467	-	0.80	Load-hold cycle 1
	-	-	636	1.09	reload to failure
106	1.25	592	517	1.01	spontaneous failure
108	180	505	-	0.86	Load-hold
109	180	546	-	0.93	Load-hold
110	0.03	564	561	0.96	spontaneous failure
112	-	-	573	0.98	load to failure
113	180	563	-	0.96	Load-hold
114	180	518	-	0.88	Load-hold
115	360	534	-	0.91	Load-hold
116	180	460	-	0.78	Load-hold
117	180	318	-	0.54	Load-hold
123	180	334	-	0.57	Load-hold
124	-	556	-	0.95	Load-hold cycle 1
	-	562	-	0.96	Reload cycle 2
	-	-	657	1.12	reload to failure
125	180	546	-	0.93	Load-hold cycle 1
	-	-	617	1.05	reload to failure

3.3 Strength and time-to failure

Figure 3 displays for each sample the holding times versus its maximum axial load. Four groups are plotted: (a) samples loaded to failure (solid squares) for which the time is arbitrarily selected as 0.1s and the shown stress is the ultimate strength; (b) load-hold samples that did not fail (solid diamonds) shown by experimental hold time and maximum load; (c) load-hold samples that fail spontaneously marked by a line connecting the stress at the start of the holding (small solid dot) and the stress during failure (large, solid dot); and (d) cycle-to-failure tests (solid dots) for which the time is arbitrarily selected as 0.1s and the shown stress is the ultimate strength.

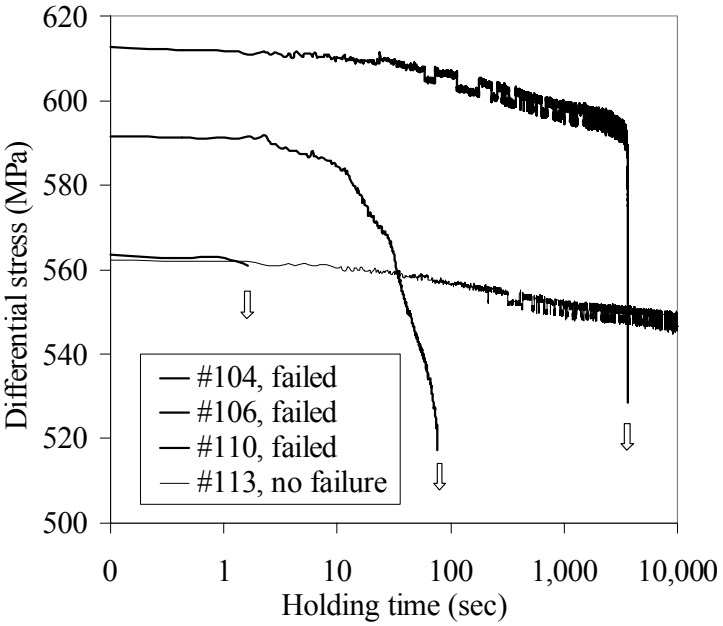

Figure 2. Differential-stress variations during the holding period of three samples that failed spontaneously (104-upper curve, 106-middle curve, 110-lower curve, all with open arrow) and sample 113 that did not fail.

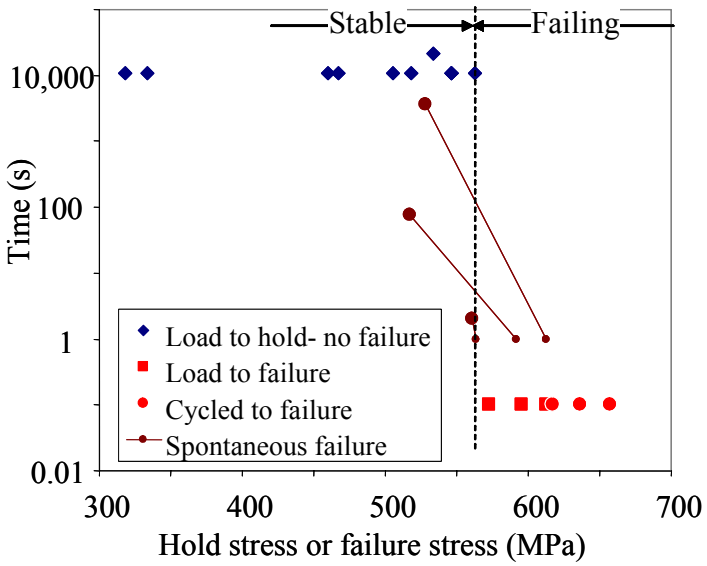

Figure 3. The hold time that is the elapsed time from start of holding period to unloading or to spontaneous failure, as function of the pre-selected load. Vertical dotted line is the critical stress (0.96 the strength, see text). Three inclined lines indicate the stress relaxation of the spontaneously failed samples (104, 106, and 110).

3.4 *Microdamage*

Our microstructural analysis covered the mode, dimensions, density and distribution of stress-induced microfractures in the deformed samples as reported by Katz (2002) and Katz & Reches (2002). The microfractures were mapped in four samples subjected to load-hold testing with maximum NDS values of 0.57, 0.88, 0.96 (unfailed) and 0.96 (failed), and one unstressed sample (123, 114, 113, 110 and 157).

The deformed specimens display two dominating microfracture groups that account to more then 80% of the mapped fractures. One group includes tensile microfractures trending subparallel to the loading axis, and the other group includes shear microfractures trending in the interval of 15°-40° off the loading axis. We note a general lengthening of the microfractures (Katz, 2002) and nonlinear increase of their density (Fig. 4); density is defined as the cumulative length of mapped microfractures per unit area (mm/mm^2).

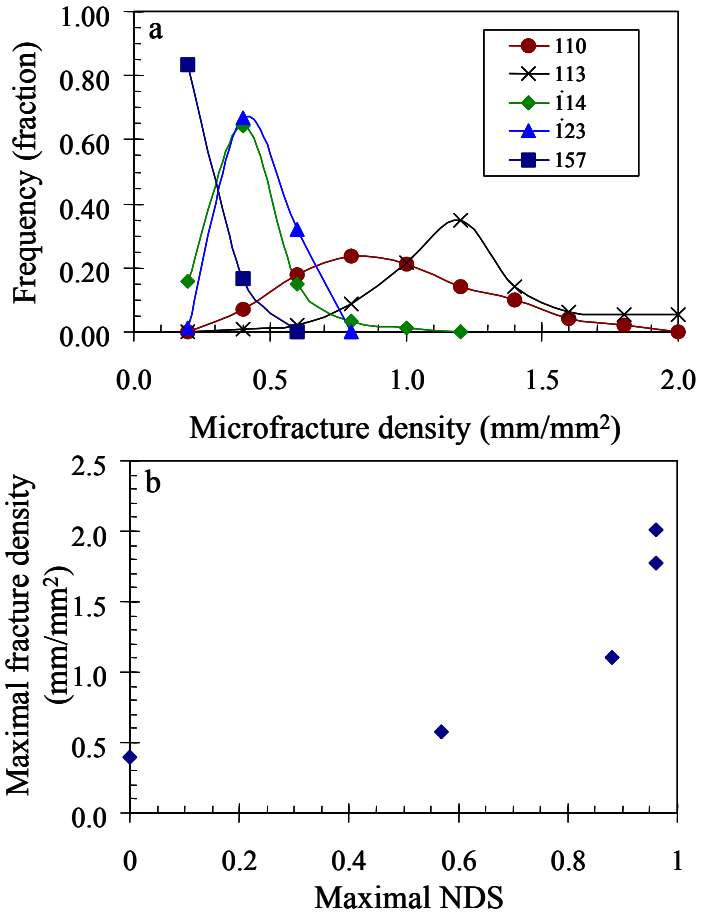

Figure 4. Measured microfracture density in deformed and undeformed samples of MSG. (a) Frequency of microfracture density in the five mapped samples. Frequency is determined on a density contour map as fraction of surface area of each density bin ($0.2mm/mm^2$ steps); the contour map is not shown. (b) Maximum fracture density as function of maximum load.

4 DISCUSSION

4.1 *A critical stress for spontaneous failure*

The present experiments indicate that for hold periods up to six hours, spontaneous failure occurs only above a critical stress of NDS ≈ 0.96 (Fig. 3), and this failure is preceded by the time-dependent creep and stress relaxation (Figs. 2, 3). The behavior above this critical stress is highly nonlinear as portrayed by the wide range of the time-to-failure (Fig. 3), the irregular style of stress relaxation (Fig. 2), the wide range of crack volume strain, CVS, for samples loaded to NDS ≥ 0.96 (Katz, 2002), and the nonlinear increase of microdamage (Fig. 4b). The delay in spontaneous failure (Figs. 2, 3) is apparently a self-induced process that requires no additional external energy (note the stress relaxation in Fig. 2).

The long-term strength of granite samples was experimentally analyzed by Schmidtke and Lajtai (1985). They conducted 140 unconfined creep tests on Lac du Bonnet granite for up to 40 days. While they concluded that the granite has a finite, long-term strength of about 0.45 the instantaneous strength, they also show that a zero long-term strength cannot be rejected. Martin and Chandler (1994) used the same data set to show that samples loaded above 0.7 the instantaneous strength would fail in less than one day. They related this critical stress to the irreversible microdamage associated with the C_{cd} load of trend reversal of the experimental volumetric strain curve in Figure 1. Lockner (1998) showed that within the time limits of experimental creep data, Westerly granite has zero long-term strength.

The results of these studies indicate that the critical stress decreases with the increase of holding time. Thus, the observed critical stress of NDS ≈ 0.96 of the MSG samples is limited to loading period of few hours.

4.2 *Strength variations*

We examined the strength variations of MSG with the Weibull distribution. While originally developed for the analysis of tensile strength in brittle solids (Lawn, 1993, Ch. 10), this distribution has been applied to analyze the shear strength of rocks (Gupta & Bergstom, 1998) and other phenomena.

This distribution predicts that the probability P for a sample to fail under differential stress U_S is

$$P = 1 - \exp\left[-\left(U_S / \sigma_0\right)^m\right]$$

where the Weibull modulus, m, and the scaling stress σ_0, are adjustable parameters. Strength values of 11 failure tests are used here (nine from the present work, Table 1, and two from Katz et al. 2001). One should note that this is a small sampling size for typical Weibull analysis (Lawn, 1993, p. 340).

We follow Lawn (1993) to calculate the Weibull probability for two sets of data. For the first we use

the strength values during actual failure, namely after the time-dependent creep of the samples (solid diamonds and linear fit for 'Time-dependent failure' in Fig. 5). For the second we use the strength values before the time-dependent creep (open squares and linear fit for 'Instantaneous failure' in Fig. 5). For this case, the values of maximum load at the start of the holding period are used.

The calculated Weibull modulus have high values ($m \approx 13$ and $m \approx 22$ for the first and second option, respectively, in Fig. 5), which are typical to reliable solids (Lawn, 1993). Finally, the fairly clear linear fit for both options (Fig. 5) suggests a well-behaving population of pre-failure microfractures (Lawn, 1993), in agreement with our microstructural observations (Fig. 4) (Katz & Reches, 2002).

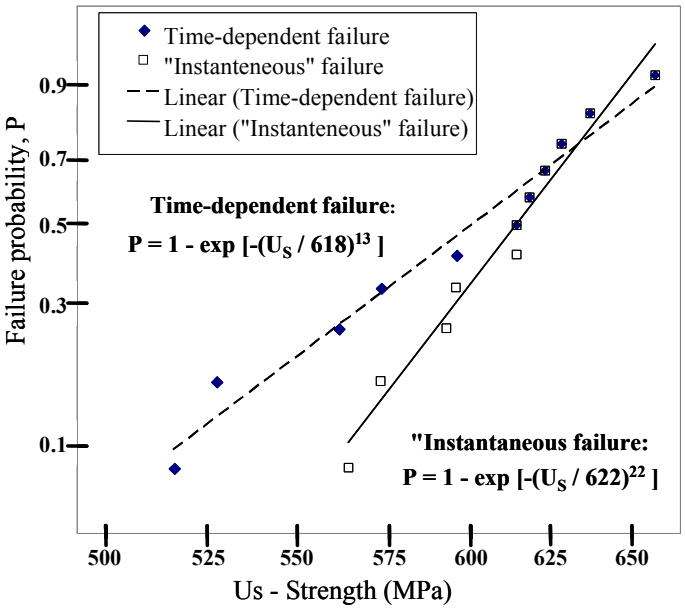

Figure 5. Strength variations of MSG samples plotted on Weibull diagram (after Lawn, 1993). The two sets of data that are plotted are described in the text.

5 CONCLUSIONS

(1) The spontaneous failure of Mount Scott granite occurs above a critical stress of about 95% of its ultimate rock strength for the present conditions. Above this stress the damage increases nonlinearly even when the load spontaneously relaxes and the sample creeps.

(2) The pre-failure damage includes shear and tensile microfractures in approximately equal amounts. The shear microfractures are significantly longer in the later stages of the deformation.

(3) The Weibull distribution parameters of the strength data of Mount Scott granite indicate a well-behaving damage population.

6 ACKNOWLEDGEMENTS

The laboratory work was conducted at the Rock Mechanics Institute, University of Oklahoma, Norman, with the help and advice of J-C. Roegiers, Gene Scott and Pete Keller.

The study was supported, in part, by Eberly Family Chair funds of M. Charles Gilbert, the Rock Mechanics Institute, University of Oklahoma, Norman, the US-Israel BiNational Science Fund, grant 98-135 and the Geological Survey of Israel project 30225.

7 PREFERENCES

Ashby, M., F., Hallam, S., D., 1986, The failure of brittle solids containing small cracks under compressive stress states. *Acta Metall., 34, 497-510*.

Hadley, K. 1976. Comparison of calculated and observed crack densities and seismic velocities in Westerly Granite. *J. Geophys. Res, 81,* 3484-3494.

Gupta, V., Bergstrom, J. S. 1998. Compressive failure of rocks by shear faulting. *J. Geophys. Res. 103*, 23875-23895.

Katz, O. 2002. Mechanisms of faults nucleation in brittle rocks. *Ph.D. dissertation, Hebrew University, Jerusalem.*

Katz, O. Gilbert, M. C. Reches, Z. Roegiers, J. C. 2001. Mechanical properties of Mount Scott granite, Wichita Mountains, Oklahoma. *Oklahoma Geology Notes, 61 (2)*, 28-34.

Katz, O., Reches, Z. Microfracturing, damage and failure of brittle granites. *Submitted to J. Geophys. Res.* (May, 2002).

Lawn, B., 1993. *Fractures of brittle solids-Second edition*. Cambridge University press.

Lockner D. A., 1998, A generalized law for brittle deformation of Westerly granite, *J. Geophys. Res.,* 103, 5,107-5,123.

Lockner D. A., Moore D. A., Reches Z. 1992. Microcracks interaction leading to shear fracture, in Tillerson and Wawersik (eds), *Rock Mechanics,* Rotterdam: Balkema.

Lyakhovsky V., Z. Reches, R. Weinberger, and T. E. Scott, 1997, Non linear elastic behavior of damaged rocks. *Geophys. J. International*, 130, 157-166.

Martin, C. D., Chandler N. A. 1994. The progressive fracture of Lac du Bonnet granite. *Int. J. Rock Mech. Min. Sci. Geomec. Abst., 31,* 643-659.

Price, J. D., Hogan J. P., Gilbert M. C. 1996. Rapakivi texture in the Mount Scott granite, Wichita mountains, Oklahoma, *European Journal of Mineralogy, 8, 2*, 435-451.

Reches, Z., Lockner D. A. 1994. The nucleation and growth of faults in brittle rocks. *J. Geophys. Res., 99,* 18,159-18,174.

Salganik., R., L., Rapoport, I., Gotlib, V.,A., 1994. Delayed fracture in brittle wear: an approach. *International J of Fracture v. 68,* 65-72.

Schmidtke R. H., Lajtai E.Z., 1985, The long-term strength of Lac du Bennet granite, *Int. J. Rock Mech. Min Sci. Geomech. Abstr,* 22, 461-465.

Tapponnier, P., Brace W. F. 1976. Development of Stress-Induced Microcracks in Westerly Granite, *Int. J. Rock Mech. Min Sci. Geomech. Abstr., 13*, 103-112.

Wawersik, W. R., Brace W. F. 1971. Post-failure behavior of a granite and diabase, *Rock Mechanics, Supplementum, 3; 2,* 61-85.